ASM Handbook, Volume 19: Fatigue and Fracture
ASM Handbook Committee, p 381-392
DOI: 10.1361/asmhba0002379

Fracture Resistance of Structural Alloys

K.S. Ravichandran, The University of Utah, and A.K. Vasudevan, Office of Naval Research

FRACTURE MECHANICS is a multidisciplinary engineering topic that has foundations in both mechanics and materials science. From the perspective of a metallurgist, fracture mechanics often emphasizes mathematical mechanics, where the primary focus is on analytical methods. However, the microstructural aspects of fracture mechanics (quantified in terms of various measures of fracture toughness such as K_{Ic}, K_c, or K_{Id}) is important for several reasons. First, in many applications, fracture toughness is useful for design and/or as a quality control parameter. Secondly, fracture mechanics provides a more meaningful measure of fracture resistance in the presence of cracks or defects than other material properties such as ductility. Therefore, fracture mechanics plays a major role in both the application and the development and production of structural materials for petroleum, chemical, mining, aerospace, and naval applications.

The objective of this article is to summarize the microstructural aspect of fracture resistance in structural materials. The intent is to selectively compile and compare information on microstructure and fracture resistance of structural materials from literature and some of the author's work. The article begins with brief coverage on basic fracture principles, followed by material examples. Included in this text are examples of steels, aluminum alloys, titanium alloys, cermets, and composites. More detailed coverage is provided in other sections in this Volume.

Basic Fracture Principles

The mechanics of the fracture process (in either elastic or elastic-plastic conditions) is understood by considering a body with a crack length a subjected to an applied tensile stress σ. For purely brittle fracture originating from this crack, Griffith postulated that the critical rate of strain energy released during unstable crack extension, G_c, is related to the surface energy of the material, γ, as:

$$G_c = 2\gamma \quad \text{(Eq 1)}$$

$$G_c = \frac{\pi \sigma_c^2 a}{E} \quad \text{(Eq 2)}$$

where σ_c is the critical stress at the onset of fracture and E is the elastic modulus. From the linear elastic stress field ahead of a sharp crack, Irwin found that at regions very close to the crack tip, the stress normal to the fracture plane, σ_{yy}, is related to the stress-intensity factor, K, as:

$$\sigma_{yy} \approx \frac{K}{\sqrt{2\pi r}} \quad \text{(Eq 3)}$$

where $K = \sigma\sqrt{\pi a}$, σ is applied stress, and r is the distance from the crack tip on the crack plane. K is a measure of buildup or concentration of stress at the tip of a sharp crack. If fracture occurs from the crack, then the local critical value of σ_{yy} at which fracture occurs (e.g., by cleavage) is reflected as the critical value of K. Irwin further showed that K and the strain energy release rate, G, are related as:

$$G = \frac{K^2}{E} \quad \text{(Eq 4)}$$

It then follows that fracture will occur from the crack when the critical stress intensity at the crack tip, $K = K_c$, is reached, corresponding to $G = G_c$. Due to this simplicity, K_c has been accepted as a useful parameter representing fracture resistance of materials in engineering applications.

If the crack size is much smaller than the body dimensions, the relationship between fracture toughness, K_c, and fracture stress, σ_c, can be simply written as:

$$K_c = \sigma_c\sqrt{\pi a} \quad \text{(Eq 5)}$$

However, when the size of the crack from which fracture occurs is significant in relation to body dimensions:

$$K_c = \sigma_c\sqrt{\pi a}\, F\left(\frac{a}{W}\right) \quad \text{(Eq 6)}$$

where $F(a/w)$ is a function that accounts for the effects due to the finiteness of the body and is dependent on the shape of the body. The values of these factors can be found in handbooks on fracture mechanics as well as in the ASTM standard for fracture toughness testing, E 399. The appendix of this Volume also contains updated information on geometry factors, $F(a/W)$.

The above fracture relationships are strictly applicable to brittle materials in which the energy dissipation due to plastic deformation is almost negligible. Many structural materials, particularly those in the high-strength category, show evidence of plastic deformation and have fracture toughness levels higher than those that can be estimated from surface energy (Eq 1) alone. Hence, the modified form of Eq 1 to account for this additional contribution to fracture resistance due to plastic deformation can be written as:

$$G_c = \underset{\text{(elastic)}}{2\gamma} + \underset{\text{(plastic)}}{\Gamma \sigma_y \delta_c} \quad \text{(Eq 7a)}$$

or in terms of fracture toughness:

$$K_c = \sqrt{2E\gamma + \Gamma E \sigma_y \delta_c} \quad \text{(Eq 7b)}$$

where Γ is constant, σ_y is the material yield stress, and δ_c is the critical opening displacement at the crack tip at the onset of fracture. The first term is the energy consumed in the creation of two fracture surfaces during fracture and is considered to be independent of microstructure. The second term, $\sigma_y\delta_c$, represents approximately the energy consumed in plastic deformation accompanying fracture, a strong function of microstructure. Because the latter is several times higher than the former, the surface energy term is often ignored in the case of metallic structural materials.

From Table 1 it is evident that crack-tip plasticity accounts for much of the fracture resistance of structural metals. This fact makes it possible to alter microstructure for optimizing fracture resistance, through variables that influence strength and ductility, such as strain hardening, dislocation-particle interactions, and slip behavior. The mechanism of crack propagation depends on microstructural features as classified by Schwalbe (Fig. 1). This forms the basis of the discussion on individual alloys later. Further, due to an increase

Table 1 Fracture toughness values estimated from interfacial energies and the measured fracture toughness values of alloys

Material	Interfacial energy (2γ), dynes/cm^2	G_{Ic}, MPa · m	E, MPa	K_{Ic}, MPa$\sqrt{m}$ (a)	K_{Ic}, MPa$\sqrt{m}$ (b)
α-Fe	4000	0.0004	200,000	8.9	20-150
Ti	2300	0.00023	100,000	4.8	30-80
Al	1350	0.00014	70.000	3.0	20-60

(a) Estimated. (b) Measured for alloys

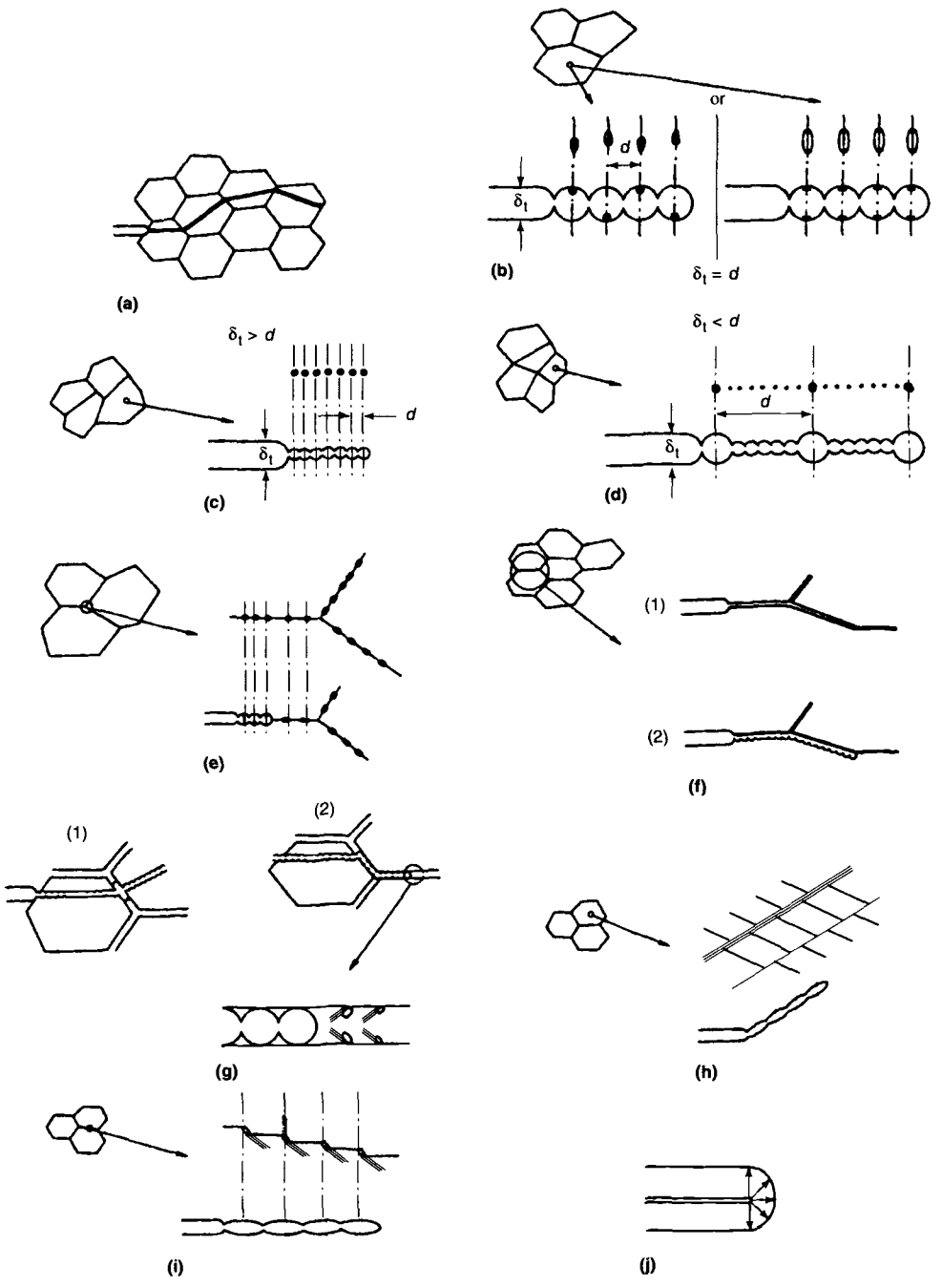

Fig. 1 Crack propagation mechanisms: (a) Cleavage crack propagation. (b) Dimple fracture due to coarse particles. (c) Dimple fracture due to fine particles. (d) Dimple fracture due to coarse and fine particles. (e) Intergranular crack propagation due to grain boundary precipitates. (f) Intergranular crack propagation due to a hard phase grain boundary film. (g) Crack propagation mechanisms when a soft phase grain boundary film is present .(h) Crack propagation by slip plane/slip plane intersection. (i) Crack propagation by slip plane/grain boundary intersection. (j) Crack propagation solely by plastic blunting

in elastic modulus, the ranges of fracture toughness values obtainable by microstructure manipulation increases in the order of aluminum alloys, titanium alloys, and iron alloys (Fig. 2).

Fracture toughness values for materials are obtained by testing precracked compact tension or three-point bend specimens, following the ASTM E 399 test procedure. A measure of fracture resistance can also be obtained from Charpy specimens used in impact toughness testing. However, for comparison with linear elastic fracture mechanics specimens, precracked specimens are often used. Figure 3 illustrates the correlation between the critical strain energy release rates for fracture (K_{Ic}^2/E) and total energy absorbed per unit fracture area of precracked Charpy specimens, tested in slow bending, for different materials. This confirms that the critical strain energy release rate represents the energy required to cause fracture, even in the presence of plastic deformation. An approximate measure of this can also be obtained from simple Charpy specimens, as an alternative to the ASTM standard for fracture toughness test procedure.

Fracture Resistance of High-Strength Steels

Although engineering applications use many types of steels (such as mild steels, high-carbon steels, and alloy steels), only high-strength alloy steels are described in this article because of the general inverse relationship between strength and fracture toughness (Fig. 4). Examples of such steels include high-strength low-alloy steels, tool steels, dual-phase steels, maraging steels, and precipitation-hardenable stainless steels. The development of strength and toughness in these steels is linked to such factors as the size and distribution of carbides and nitrides, relative proportions of martensite and austenite phases, and grain size. In general, as shown in Fig. 4, high-fracture-toughness steels have ductile (low-carbon) martensite and retained metastable austenite as dominant phases in the microstructure. Steels that contain predominantly ferritic and pearlitic structures have relatively low fracture toughness. Table 2 summarizes the effects of microstructure on toughness.

Maraging (martensite-aging) steels, based on the Fe-Ni-Ti system, have very high strength and high fracture toughness and are designed with very low levels of carbon (<0.05%) and high levels of alloying elements (typically 18% Ni, 3% Ti, and 1 to 2% Co). The benefit of low carbon is twofold: crack-initiating carbides are absent and the martensite matrix is more ductile. In addition, maraging steels contain retained austenite (due to the high nickel content), which causes extensive plastic deformation and strain-induced martensitic transformation at the crack tip during fracture, thus increasing the fracture resistance. The strengthening lost by the elimination carbides is

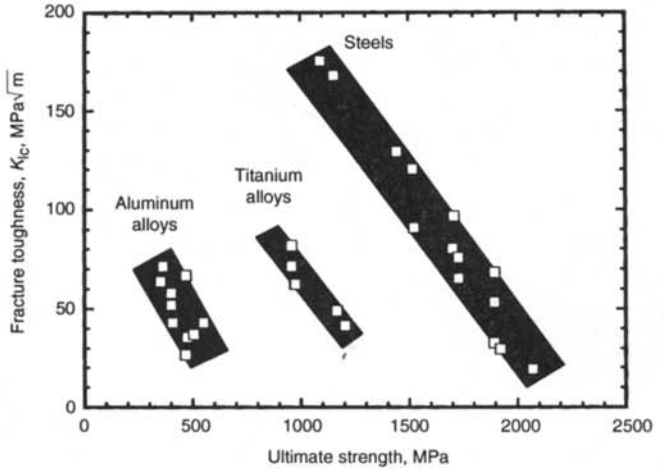

Fig. 2 Fracture toughness as a function of strength for high-strength structural alloys

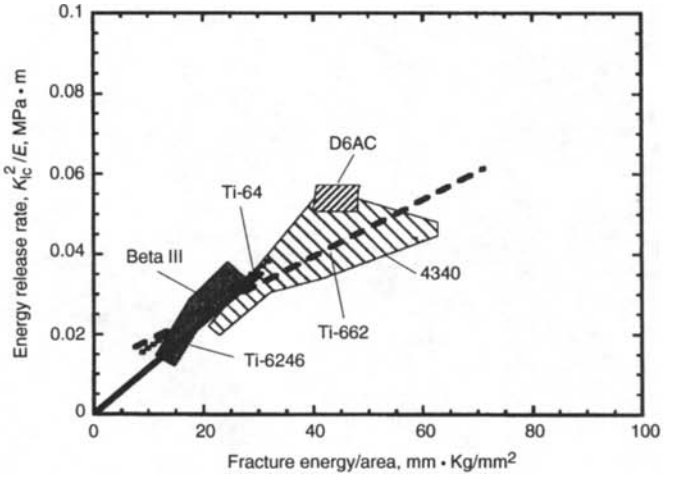

Fig. 3 The correlation between energy release rate and fracture energy of Charpy specimens for various materials

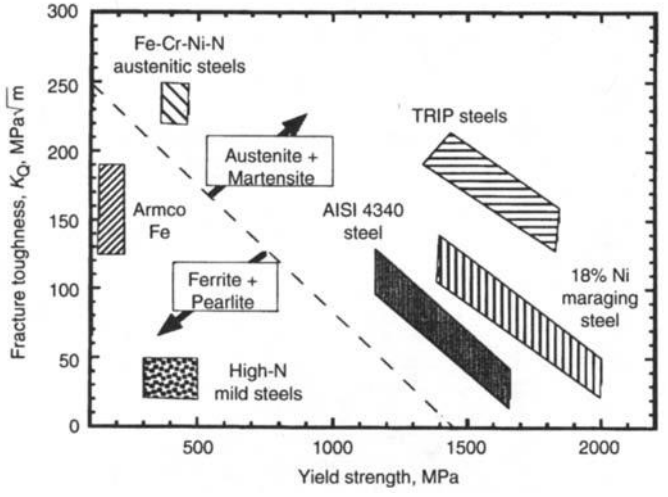

Fig. 4 Fracture toughness as a function of yield strength for structural steels. TRIP, transformation-induced plasticity

Table 2 Effects of microstructural variables on fracture toughness of steels

Microstructural parameter	Effect on toughness
Grain size	Increase in grain size increases K_{Ic} in austenitic and ferritic steels
Unalloyed retained austenite	Marginal increase in K_{Ic} by crack blunting
Alloyed retained austenite	Significant increase in K_{Ic} by transformation-induced toughening
Interlath and intralath carbides	Decrease K_{Ic} by increasing the tendency to cleave
Impurities (P, S, As, Sn)	Decrease K_{Ic} by temper embrittlement
Sulfide inclusions and coarse carbides	Decrease K_{Ic} by promoting crack or void nucleation
High carbon content (>0.25%)	Decrease K_{Ic} by easily nucleating cleavage
Twinned martensite	Decrease K_{Ic} due to brittleness
Martensite content in quenched steels	Increase K_{Ic}
Ferrite and pearlite in quenched steels	Decrease K_{Ic} of martensitic steels

replaced by precipitation of fine $(Fe,Ni)_3Ti$ phases from martensite, obtained by aging. However, under certain conditions, precipitation of phases at grain boundaries leads to deterioration in toughness. Hence, chemistry, processing, and heat treatment conditions should be designed to avoid the grain boundary precipitation. Typical heat treatment of a maraging steel involves austenitization and oil quenching or air cooling, followed by aging at high temperature in the $\alpha + \gamma$ field.

Metastable Austenite-Based Steels. Transformation-induced plasticity (TRIP) steels with high contents of nickel and manganese retain high-temperature face-centered cubic austenite (γ) at room temperature, upon quenching. By a judicious choice of composition, this austenite is designed to be metastable after quenching and transformable during deformation. The deformation and the volume change accompanying the austenite-to-martensite transformation increase the energy required for extension of a moving crack, resulting in high fracture toughness. The fracture toughness of such steels depends on the stability of austenite, measured in terms of the transformation coefficient, m, in the following relationship between the volume fraction of martensite formed (V_α) and tensile strain (ε):

$$V_\alpha = m\sqrt{\varepsilon} \qquad \text{(Eq 8)}$$

The higher the tensile strain or crack opening displacement at the tip, the larger the volume fraction of transformed martensite and the higher the TRIP effect on toughness, as illustrated in Fig. 5. These steels possess the highest fracture toughness levels attainable in steels and hence are used in mining, drilling, and other applications requiring wear and erosion resistance.

Quenched-and-Tempered Steels. Fracture resistance in quenched-and-tempered steels is achieved by eliminating coarse alloy carbides, increasing hardenability to minimize ferrite formation, and alloying to retain austenite at room temperature.

An increase in the austenitization temperature, besides coarsening the grain size, dissolves carbides and nitrides present in steels. This eliminates the crack nucleation from carbides, thereby increasing the fracture toughness, as shown in Fig. 6 for two steels. The required austenitization time is also critical, and both time and temperature are chosen according to the amount of carbon and alloying elements in the steel. The effect of tempering temperature on fracture toughness depends on the type of prior austenitization treatment (Fig. 7). For example, the heat treatment involving austenitization at 1200 °C (2190 °F), followed by an ice brine quench and refrigeration in liquid nitrogen, results in high fracture toughness levels at all tempering temperatures, compared to austenitizing at 870 °C (1600 °F) and quenching in oil. The higher fracture toughness

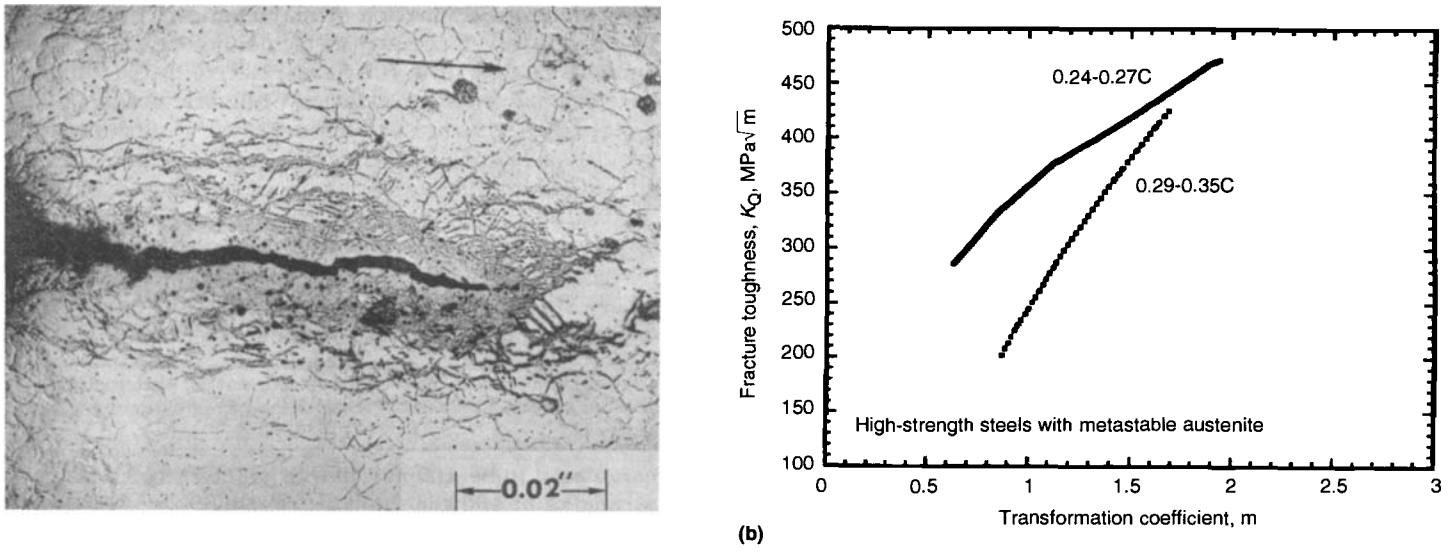

Fig. 5 TRIP steel crack and toughness. (a) Formation of martensite around a crack in a TRIP steel. (b) The effect of austenite transformation on the fracture toughness of metastable austenitic steels

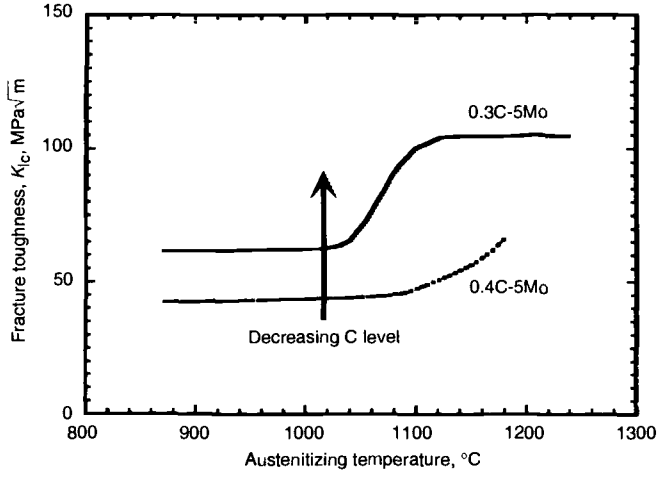

Fig. 6 The effect of austenitization temperature on the fracture toughness of two quenched-and-tempered steels

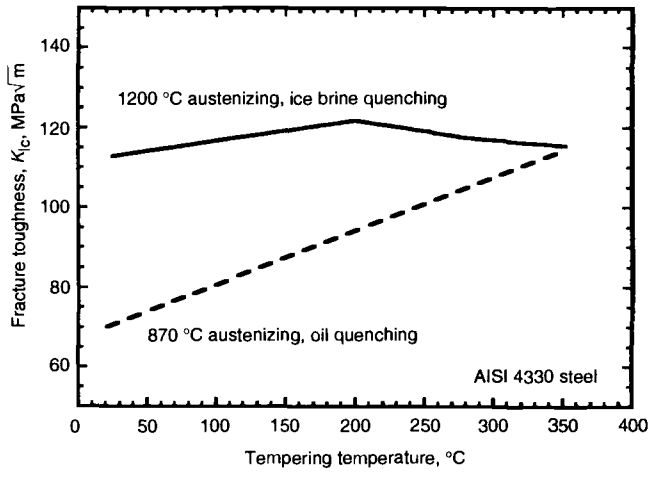

Fig. 7 The effect of tempering temperature on fracture toughness

levels of the former is attributed to the formation of 100% refined martensite upon quenching. Heat treatment at 870 °C (1600 °F) results in a mixture of blocky ferrite and upper bainite having continuous films of carbides at lath boundaries. This leads to low fracture toughness due to easy crack propagation along the lath boundaries at low tempering temperatures. However, at higher tempering temperatures, elimination of continuous carbide film by spheroidization increases the fracture toughness. In addition, in some alloy steels, retained austenite contributes to further increases in fracture toughness, by either crack-tip blunting or strain-induced transformation.

Fracture toughness in steels also depends on the nature of martensite (low-carbon ductile martensite or high-carbon twinned martensite). Supersaturated carbon in martensite increases the twinning to accommodate the strains in iron lattice due to carbon. The low fracture toughness levels of some martensitic steels at low tempering temperatures are due to the presence of brittle twinned martensite. An increase in the twin density of martensite results in low fracture toughness, as shown in Fig. 8.

Inclusions decrease fracture toughness (Fig. 9) by promoting crack nucleation by inclusion fracture, void nucleation at the particle-matrix interface, and early coalescence. This reduces the extent of void growth before fracture, limiting the plastic energy absorption in the process zone at the crack tip. A decrease in sulfur level in steel increases the spacing between the inclusions, thereby increasing the size of the plastically deformed process zone. This contribution to increased fracture toughness can be rationalized in terms of Kraft's model:

$$K_{Ic} \approx \sqrt{2\pi E n d_T} \qquad \text{(Eq 9)}$$

where n is the monotonic strain hardening exponent and d_T is the size of the process zone at the crack tip, proportional to the spacing between crack/void nucleating inclusions.

Fracture Resistance of Aluminum Alloys

Aluminum alloys based on Al-Cu (2*xxx* series), Al-Mg-Si (6*xxx* series), Al-Zn-Mg (7*xxx* series), and, recently, Al-Li (8*xxx* and 209*x* series) are the predominant age-hardenable alloys, used extensively in aerospace and other medium- to high-strength structural applications. Typical examples are alloys 2024, 2124, 6061, 7075, 7150, 7475, 8090, and 2091. Due to complex chemistry, precipitation, and intermetallic compound formation in aluminum alloys, control of the size and distribution of age-hardening coherent pre-

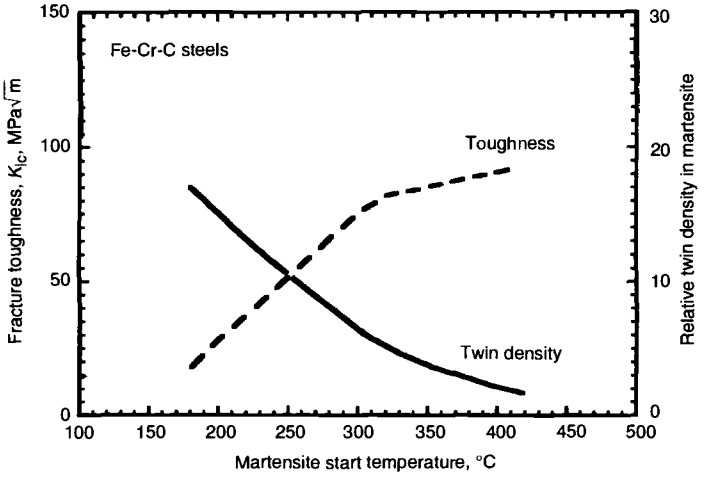

Fig. 8 Fracture toughness and martensite twin density as a function of martensite start temperature for an Fe-Cr-C steel

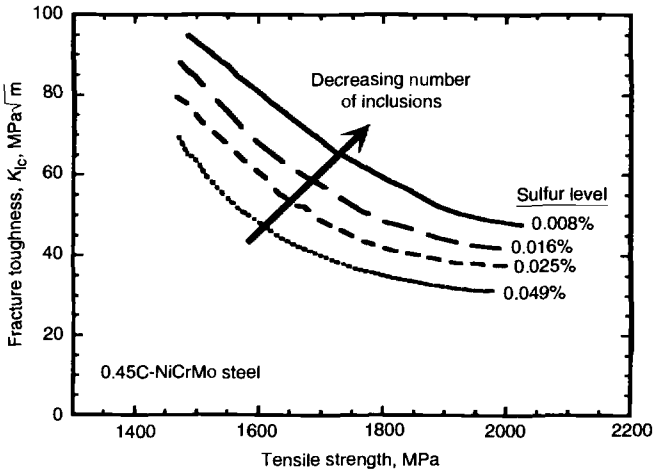

Fig. 9 The effect of sulfur on the fracture toughness vs. strength relationship

Table 3 A list of precipitates and intermetallic compounds in aluminum alloys

Precipitate phases (beneficial)	Intermetallic compounds (detrimental)
Al_2Cu	Al_7Cu_2Fe
Al_2CuMg	Mg_2Si
$MgZn_2$, Mg_2Si	$Al_{12}Mn_2Cr$
$Al_2Zn_3Mg_3$	$Al_{20}Cu_2Mn$
Al_3Zr, Al_3Li	(Fe, Mn)Al_6

Table 4 Strength and fracture toughness levels for selected aluminum alloys

Alloy	0.2% yield strength, MPa	K_{Ic}, MPa$\sqrt{m}$
2014-T6	436	20
2024-T851	443	21
2124-T851	435	26
7075-T7351	391	31
7079-T651	502	27

Table 5 Effects of processing/microstructural variables on the fracture toughness of aluminum alloys

Variable	Effect on fracture toughness
Quench rate	Decrease in K_{Ic} at low quench rates
Impurities (Fe, Si, Mn, Cr)	Decrease in K_{Ic} with high levels of these elements
Grain size	Decrease in K_{Ic} at large grain sizes due to coarse grain boundary precipitation
Grain boundary precipitates	Increase in size and area fraction decrease K_{Ic}
Underaging	Increases toughness
Peak aging	Increases fracture toughness
Overaging	Decreases fracture toughness
Grain boundary segregates (Na, K, S, H)	Lower fracture toughness in Al-Li alloys

cipitates and incoherent intermetallic phases is critical in achieving a balance of strength and resistance to fracture and stress-corrosion cracking. Table 3 lists some important precipitate phases and intermetallic compounds that form in aluminum alloys. While the precipitates control strength, intermetallic compounds that form during solidification primarily control ductility and fracture toughness.

Typical heat treatment of an aluminum alloy involves solution treatment, quenching in water, and aging at a suitable temperature for a specified period of time. Additionally, warm or cold working, such as stretching after solution treatment, is performed to control the size and distribution of precipitates. Such thermomechanical processing routes for high-strength aluminum alloys have been well developed to impart desirable combinations of strength, ductility, fracture toughness, and stress-corrosion cracking resistance.

Fracture resistance in aluminum alloys is strongly sensitive to purity, aging, the presence of intermetallic compounds, thermomechanical treatment, grain size, and orientation or texture. Typical fracture toughness values of selected aluminum alloys are given in Table 4. Table 5 gives a list of variables and the nature of their effect on the fracture toughness of aluminum alloys.

Figure 10 illustrates the effects of intermetallic-forming elements (Cr, Zr, Fe, Si, and Mn) on fracture in terms of the relationship between fracture resistance (measured in terms of the unit propagation energy in fracturing a notched bar) and tensile yield strength for two different orientations of crack propagation. Zirconium addition is beneficial due to the grain-refining effect of Al_3Zr phase. Chromium and manganese primarily lead to intermetallic compound formation and hence must be reduced to achieve a combination of high fracture toughness and high strength. Most of the intermetallic compounds form at grain boundaries in wrought alloys and at interdendritic regions in cast alloys. This is the primary reason for lower levels of fracture toughness, especially when a crack propagates in the short transverse plane (plane of rolling), in which the grain boundary area intersected by the crack plane is high compared to other orientations.

The detrimental effect of intermetallic particles on fracture toughness can be understood from a simple relationship. The critical fracture strain, ε_c, of a ligament between the crack tip and a crack/void nucleating particle is related to the particle volume fraction, V_f, as:

$$\varepsilon_c = f\left(\frac{1}{V_f}\right) \qquad \text{(Eq 10)}$$

The fracture toughness of aluminum alloys is related to the critical fracture strain as:

$$K_{Ic} \approx \sqrt{\frac{2\,C\,E\,\varepsilon_c\,\sigma_y\,n}{(1-\nu^2)}} \qquad \text{(Eq 11)}$$

where C is a constant and ν is the Poisson's ratio. As the volume fraction of brittle intermetallic particles is reduced, fracture toughness increases. For a given volume fraction of particles, fracture toughness also increases with increase in yield strength and the strain-hardening exponent of the matrix. From Eq 11, fracture toughness levels of several aluminum alloys can be predicted (Fig. 11) with good accuracy.

Figure 12 shows the effect of grain size on the fracture toughness of a 7*xxx* alloy tested with crack propagation in the long transverse direction. The decrease in fracture toughness is attributed to the increase in grain boundary fracture at large grain sizes. The increased intergranular fracture also coincides with the thickening of precipitates (e.g., the size of $MgZn_2$ precipitates in Fig. 13) at grain boundaries under prolonged aging. This behavior is also reflected in the change in fracture mode from transgranular to

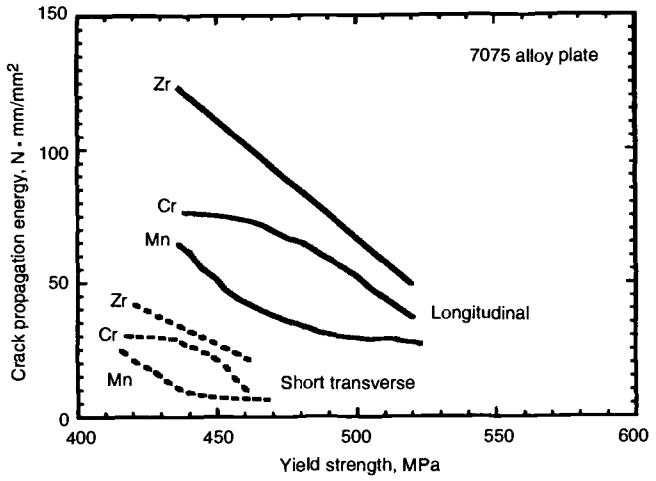

Fig. 10 The effect on toughness of elements that form intermetallic compounds

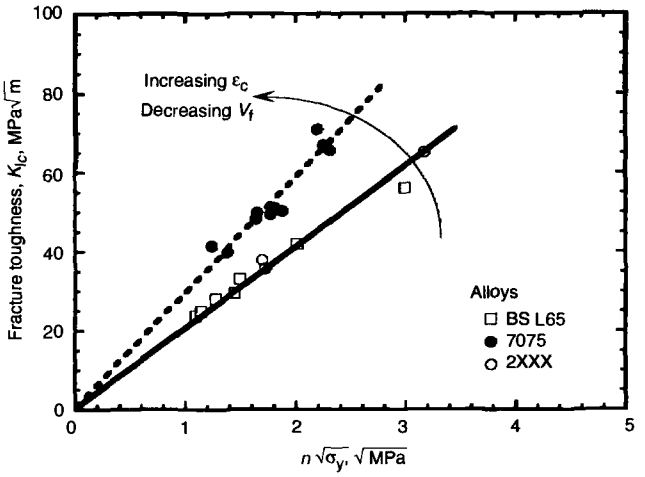

Fig. 11 The effect of parameter, $n\sqrt{\sigma_y}$ on the fracture toughness of aluminum alloys

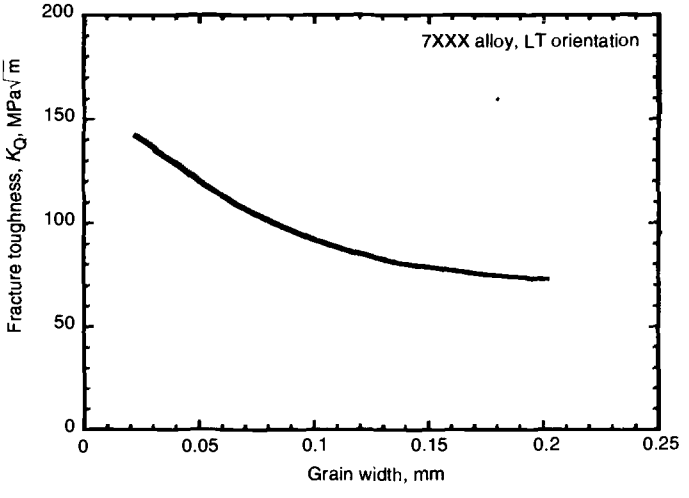

Fig. 12 The effect of grain size on the fracture toughness of a 7*xxx* alloy

intergranular. This suggests that reduced grain boundary area accompanied by coarse grain boundary precipitation is detrimental to the fracture toughness of aluminum alloys.

Figure 14 shows the broad range of data of fracture toughness and yield strength for both 2*xxx* and 7*xxx* alloys as affected by the degree of aging. Overaging generally results in low fracture toughness levels for a given yield strength and alloy type, compared with underaging. This is attributed to the increased occurrence of intergranular failure, consistent with the observations illustrated in Fig. 12 and 13.

The variables influencing fracture toughness of Al-Li alloys are similar to those that affect other age-hardenable aluminum alloys. These include degree of aging, area fraction of grain boundary precipitates, impurities, and orientation. However, Al-Li alloys are more anisotropic due to strong texture formation, relative to aluminum alloys, and hence they show a much stronger sensitivity of fracture toughness to orientation.

Fracture Resistance of Titanium Alloys

Titanium alloys are primarily used in aerospace applications owing to their good combination of specific strength, ductility, and fracture toughness. As in steels and aluminum alloys, this combination is achieved by careful control of two-phase microstructures. Among the two phases (α and β), β is more ductile and is preferable in increasing the fracture toughness of titanium alloys. The three broad classes of titanium alloys are near-α, α + β, and β alloys, grouped according to the levels of α or β stabilizing elements. Typically, β content by volume is: near-α, <10%; α + β, 10-25%; and β, >25%. Figure 15 shows the fracture toughness/strength relationship maps for different titanium alloys. Metastable β alloys possess the highest combination of strength and toughness. This arises from a large volume fraction of β phase and fine aged-α precipitates.

Table 6 Fracture toughness levels of Ti-6Al-4V alloy in different microstructural conditions

Microstructure	0.2% yield strength, MPa	Elongation, %	K_{Ic}, MPa$\sqrt{m}$
β-processed (aligned lamellar α)	903	12	78
α+β processed (equiaxed α in aged β matrix)	917	16	53
Recrystallized (fully equiaxed α)	925	19	47

Unlike steels and aluminum alloys, titanium alloys are generally free from inclusions and intermetallics that form during solidification. Neither is there precipitation and coarsening of brittle phases, so the control of microstructure for fracture toughness is less difficult. Microstructure plays a major role in controlling the fracture toughness of titanium alloys. Microstructure control is primarily achieved by mechanical processes, such as hot/cold working and heat treatment involving solution treatment followed by quenching and aging or slow cooling. Table 6 lists the fracture toughness values of a typical titanium alloy under different microstructural conditions. In general, for a given β phase content, fracture toughness increases with an increase in the amount of lamellar α as well as an increase in the aspect ratio of α phase.

The dominant variables that influence fracture toughness in titanium alloys are the interstitial elements, grain size, microstructural morphology, and relative proportions of α and β phases. Table 7 lists these variables and the nature of their effect on fracture toughness.

Figures 16 and 17 illustrate that increases in oxygen and hydrogen levels in Ti-6Al-4V alloy decrease fracture toughness. This is caused by an increase in the planarity slip, promoted by the ordering of Ti_3Al phase, which causes easy crack nucleation at grain and phase boundaries. This tendency to ordering is also increased at high

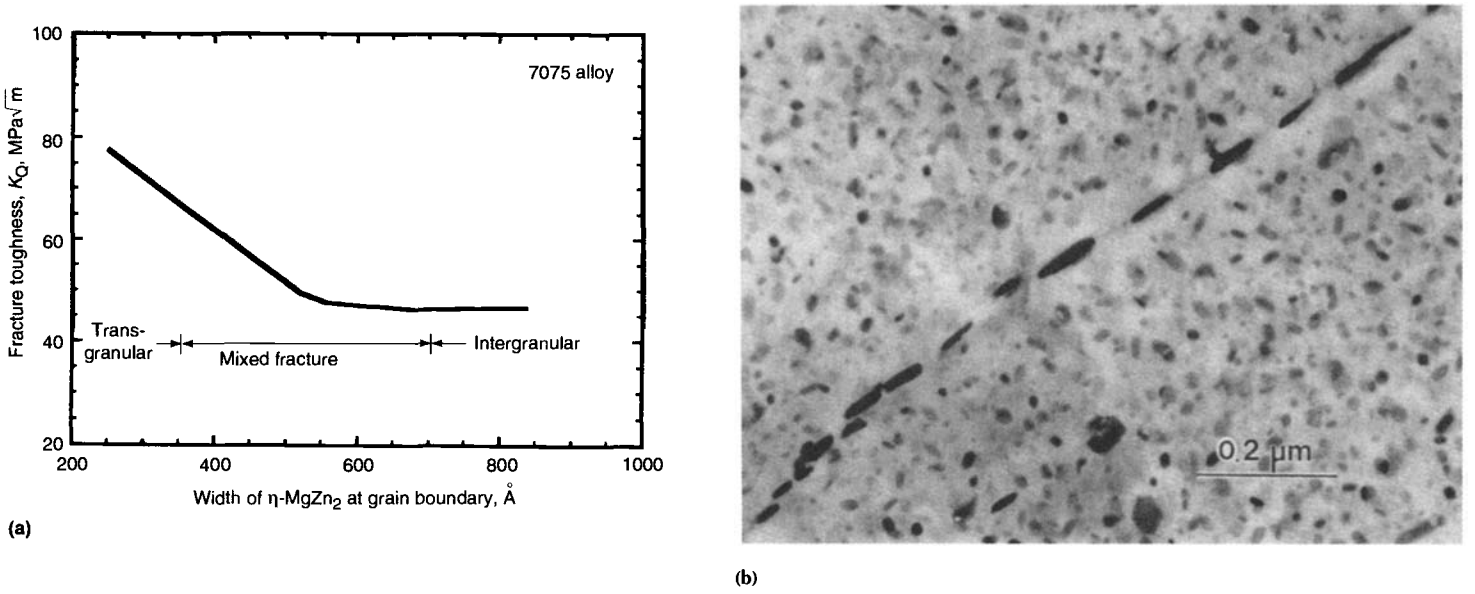

Fig. 13 7075 Al alloy. (a) The effect of grain boundary precipitate size on fracture toughness and fracture morphology. (b) Equilibrium grain boundary η-$MgZn_2$ precipitates at grain boundaries

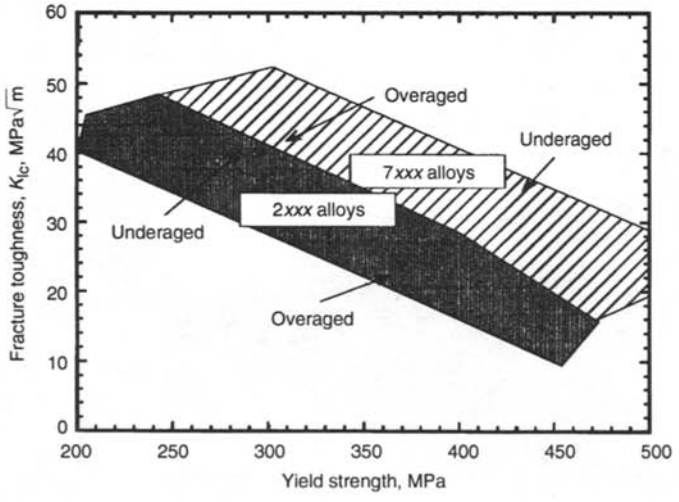

Fig. 14 The effects of alloy type and aged condition on the strength/fracture toughness relationship for aluminum alloys

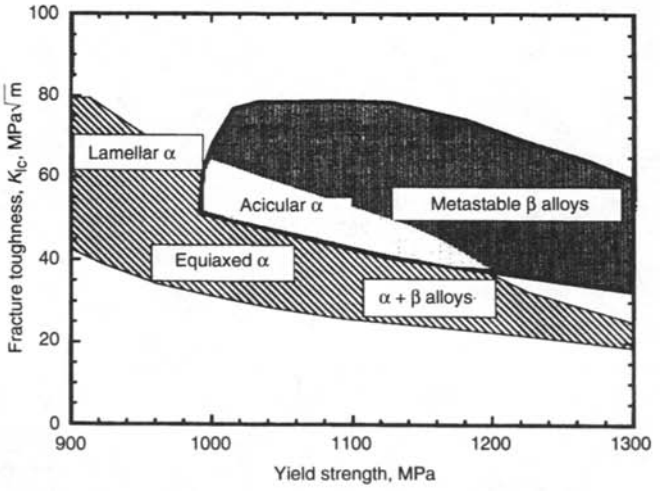

Fig. 15 The relationship between fracture toughness and strength for different classes of titanium alloys and microstructures

Table 7 Effect of microstructural variables on the fracture toughness of titanium alloys

Variable	Effect on fracture toughness
Interstitials (O, H, C, N)	Decrease in K_{Ic}
Grain size	Increase in grain size decreases K_{Ic}
Lamellar colony size	Increase in colony size increases K_{Ic}
β phase	Increases in β volume fraction, continuity increase K_{Ic}
Grain boundary α phase	Increases in thickness and continuity increase K_{Ic}
Shape of α phase	Increase in aspect ratio of α phase increases K_{Ic}
Orientation	Crack oriented for easy cleavage along basal planes gives low K_{Ic}

aluminum contents, and hence compositions of commercial alloys rarely exceed 6% Al. Hydrogen causes cleavage and interface cracking due to the formation of hydrides (TiH_2). Alloys with high levels of β phase can dissolve more hydrogen, thereby preventing the decrease in fracture toughness due to hydrogen. The other interstitial elements, carbon and nitrogen, have low solid solubility in titanium and form fine TiC and TiN dispersions when the solubility level is exceeded. These particles drastically decrease the ductility as well as the fracture toughness of titanium alloys and hence must be eliminated.

The effect of β grain size on fracture toughness is illustrated in Fig. 18 for Ti-5.2Al-5.5V-1Fe-0.5Cu alloy. There is an inverse relationship of fracture toughness to β grain size. As the grain size increases, the tendency to intergranular fracture increases, due to the weakening effect of fine 0.2 μm thick particles at the β-β grain boundary. This is primarily due to the increased density of grain boundary precipitates as a result of the reduction in available grain boundary area.

The same alloy was heat treated differently to produce thick continuous α phase at the grain boundary, which increased fracture toughness (Fig. 19). However, for this to occur, the grain interior (aged β matrix) should be stronger than α.

The orientation of crack plane in a fracture toughness test with respect to the rolling direction of the titanium alloy plate has a significant effect, due to the preferred orientation of hexagonal close-packed crystal grains having limited slip systems, relative to body-centered cubic and face-centered cubic crystals. The effect of orientation on the fracture toughness/strength relationship is illustrated in Fig. 20. While a strong inverse relationship between fracture toughness and yield strength is seen for the longitudinal orientation, it is less strong in the transverse orientation. The effect of orientation on fracture

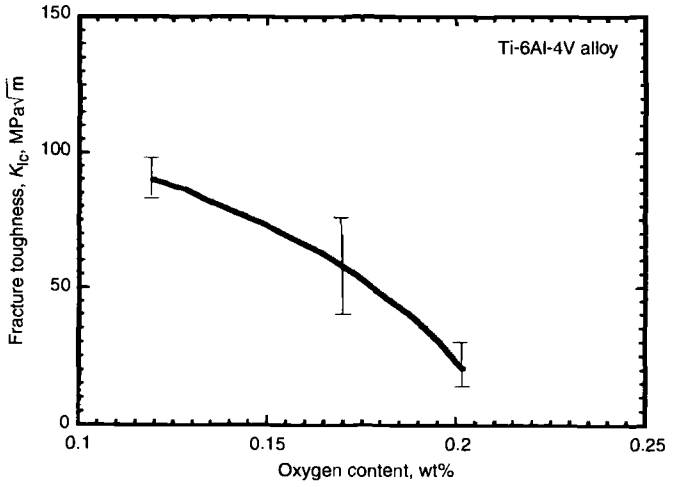

Fig. 16 The effect of oxygen level on the fracture toughness of Ti-6Al-4V alloy

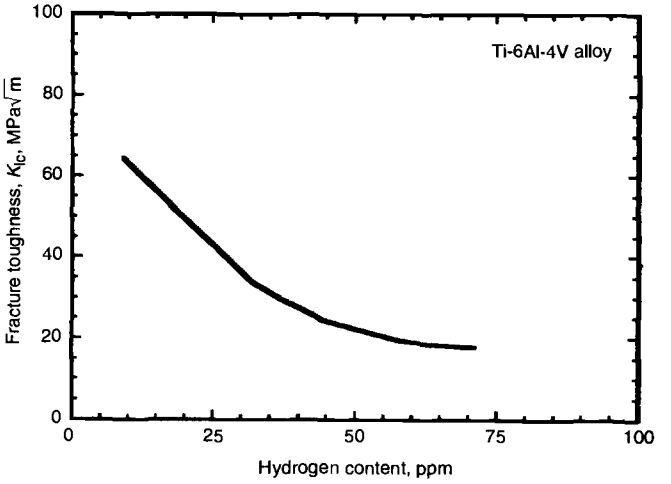

Fig. 17 The effect of hydrogen level on the fracture toughness of Ti-6Al-4V alloy

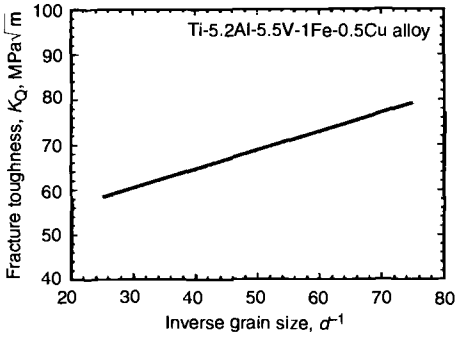

Fig. 18 The effect of grain size on the fracture toughness of a titanium alloy

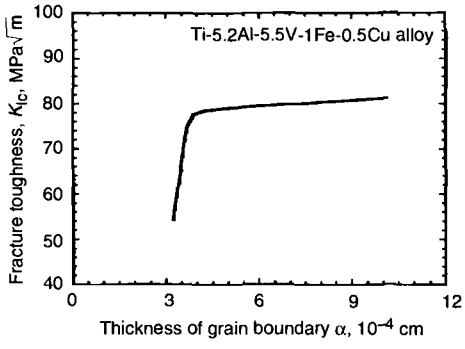

Fig. 19 The effect of the thickness of grain boundary α phase on the fracture toughness of a titanium alloy

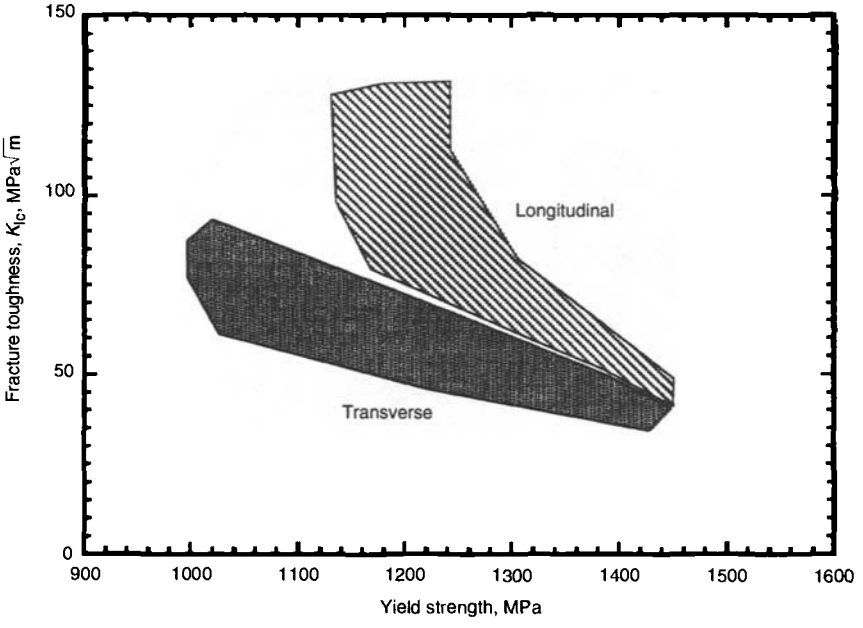

Fig. 20 The effect of crack plane orientation on the fracture toughness of Ti-6Al-4V alloy

toughness arises due to the relative orientation of slip systems such as {0001} <1120>, {1010} <1120> with respect to the crack plane. This is also evident from the variation of elastic modulus with orientation, presented in Table 8.

It is clear that the key to improving the combination of strength and toughness in titanium alloys is to increase β phase content, increase the lamellar α volume fraction and the aspect ratio of α phase, and reduce planarity of slip and interface embrittlement by reducing the levels of oxygen, hydrogen, carbon, and nitrogen.

Fracture Resistance of Composites

Brittle Matrix-Ductile Phase Composites. Ductile phases have been used to improve the fracture resistance of many structural materials, including ceramics, intermetallics, glasses, and other low-toughness materials, such as steels having a hard martensitic structure. Table 9 lists some brittle materials and the possible ductile phase reinforcements that can be used to improve the fracture toughness levels. Such an alloy design concept generally increases fracture toughness with little sacrifice in strength. The ductile phases absorb energy by plastic deformation during crack propagation. Bridging of the crack and the constrained deformation of ductile phase contribute to the increase in toughness. In general, the fracture toughness increases with an increase in the volume fraction of ductile phase (Fig. 21). For such composites, the critical strain energy release rate, G_c, for unstable fracture can be expressed as the sum of fractional energy absorbed in fracturing the brittle and ductile phases:

$$G_c = (1 - V_f)\, G_m + V_f\, \sigma_0 a_0\, \chi \qquad \text{(Eq 12)}$$

(matrix) (ductile phase)

Table 8 Effect of texture on the fracture toughness of Ti-6Al-2Sn-4Zr-6Mo alloy

Orientation	0.2% yield strength, MPa	E, MPa	K_{Ic}, MPa$\sqrt{m}$
Longitudinal	953	107,000	75
Transverse	1198	134,000	91
Short transverse	926	104,000	49

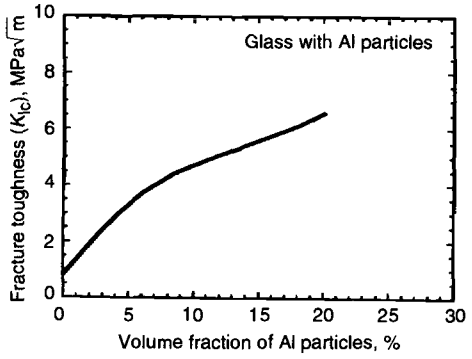

Fig. 21 Fracture toughness trend for glass having embedded ductile aluminum particles

Table 9 Brittle materials and the possible ductile phases

Material	Ductile phase
Ceramics: Al_2O_3, glass, ZrO_2, SiC, Si_3N_4	Ti, Ni, Pb, Al, Fe
Intermetallics: TiAl, NiAl, CoAl, Nb_5Si_3, Cr_3Si	Ti, Nb, Co, Mo, Cr
Martensite	Austenite, ferrite

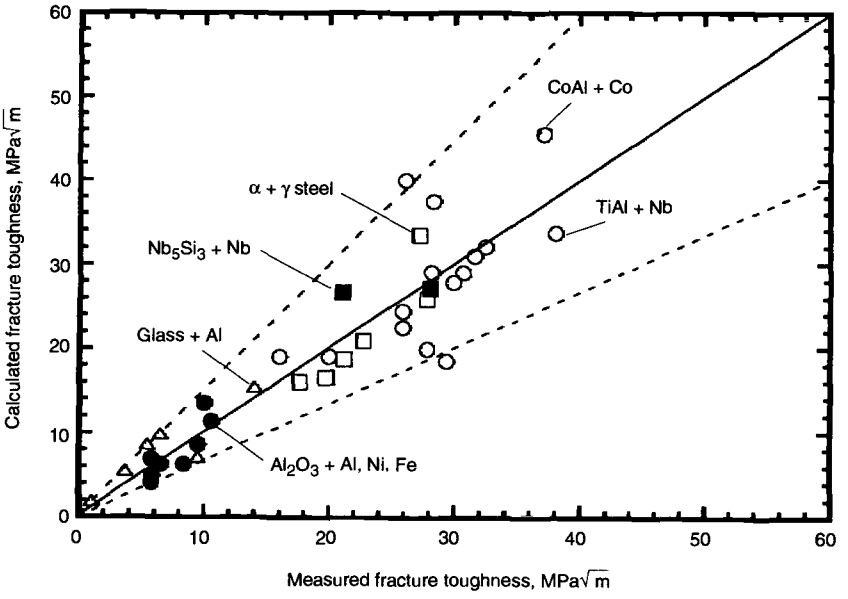

Fig. 22 The correlation between measured and calculated fracture toughness levels of several brittle materials having ductile phases as reinforcements

where σ_0 is the flow stress, a_0 is the radius of ductile phase, G_m is the energy release rate of the brittle matrix, and χ is a measure of microstructural constraint. A modified form for the above equation for the plane strain fracture toughness, K_{Ic}, can be written as:

$$K_{Ic} = \sqrt{\frac{E_c (1 - \nu_m^2) (1 - V_f) K_m^2}{(1 - \nu_c^2) E_m} + \frac{V_f E_c \sigma_0 a_0 \chi}{(1 - \nu_c^2)}} \qquad \text{(Eq 13)}$$

where E_c and ν_c are respectively the elastic modulus and the Poisson's ratio of the composite, and K_m, E_m, and ν_m are respectively the fracture toughness, elastic modulus, and Poisson's ratio of the matrix material. For the case of plane stress, $E_c/(1 - \nu_c^2)$ and $E_m/(1 - \nu_m^2)$ are to be replaced by E_c and E_m, respectively. The parameter χ (usually in the range of 2 to 6) is a measure of the constraint experienced by the ductile phase in the elastic matrix during deformation. If χ is known, in addition to matrix and particle properties, fracture toughness of the composite can be estimated with reasonable accuracy.

Figure 22 shows the correlation between the measured fracture toughness and the calculated toughness, following Eq 13. The good agreement suggests that Eq 13 adequately represents the functional dependence of fracture toughness on important microstructural parameters of the composite. Increases in the size, volume fraction, and yield strength of the ductile phase, together with an increase in composite modulus, should significantly increase the fracture toughness. The effect of Young's modulus of matrix on the composite fracture toughness is not significant. A major contribution to fracture toughness is the constraint factor, which is a measure of increase in resistance to the in situ plastic deformation of ductile phase, as imposed by the surrounding elastic matrix.

WC-Co Cermets. The case of WC-Co cermets is similar to that of the above-described ductile phase composites, except that the ductile cobalt phase surrounds the brittle WC almost completely. Figure 23 illustrates the fracture path through the cermet microstructure. The volume fraction of cobalt in these cermets is usually be-

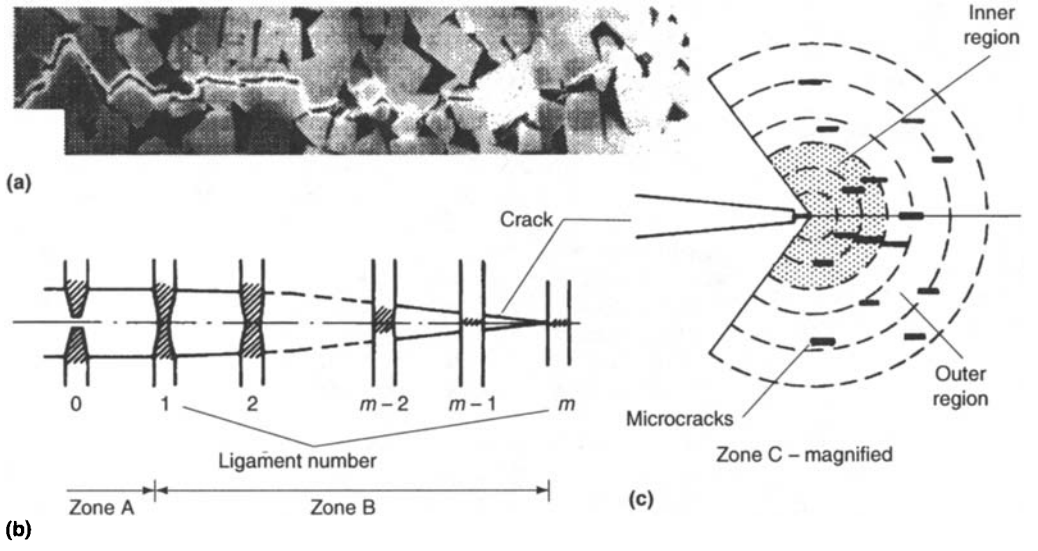

Fig. 23 Mechanisms of crack growth and fracture in WC-Co cermets

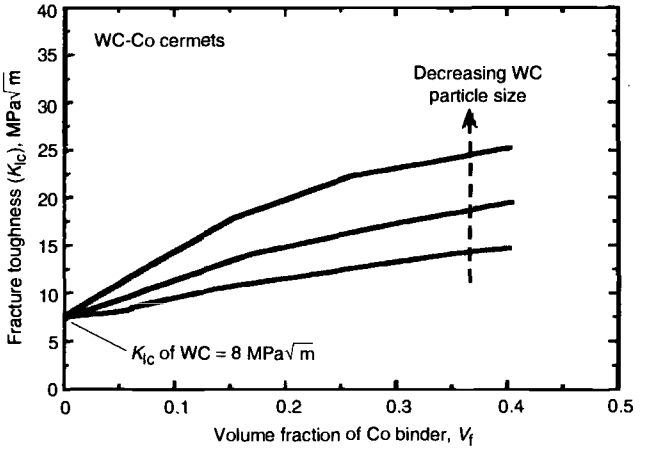

Fig. 24 The effect of ductile cobalt volume fraction and WC particle size on the fracture toughness of cermets

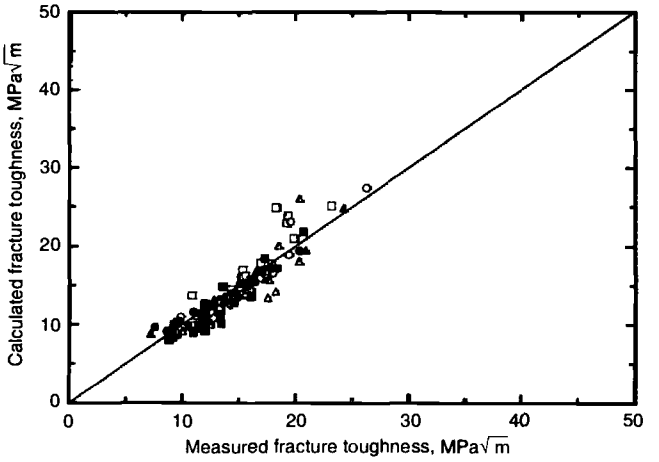

Fig. 25 The correlation between the measured and calculated fracture toughness levels of WC-Co cermets having varying sizes and volume fractions of WC and cobalt

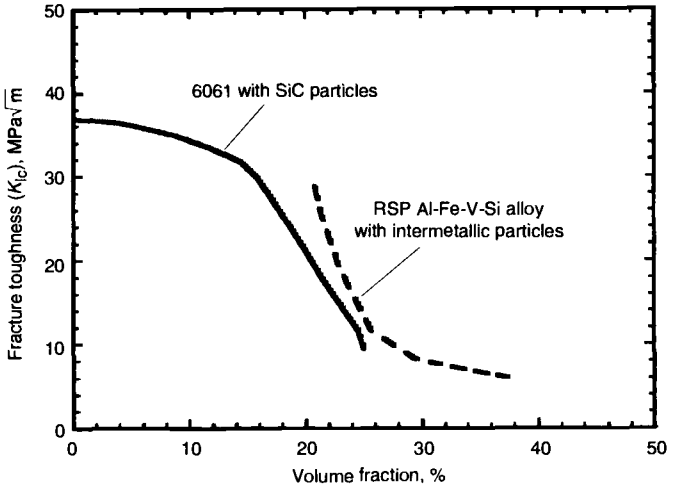

Fig. 26 The effect of dispersoids on the fracture toughness of aluminum-base metal-matrix composites

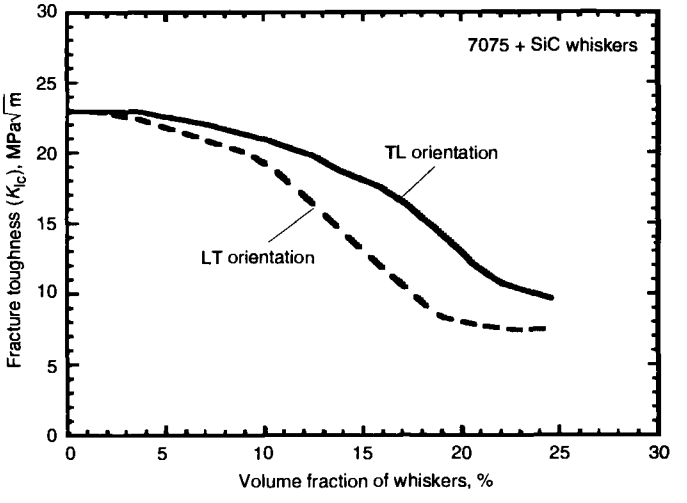

Fig. 27 The effect of orientation and whisker volume fraction on the fracture toughness of composites based on 7075 aluminum alloy

tween 0.1 and 0.3. The cermets are made by presintering WC to obtain a skeleton with continuous porosity and then infiltrating the skeleton with molten cobalt. In general, a decrease in WC particle size and an increase in cobalt volume fraction increases the fracture toughness of cermets (Fig. 24). Because of the thin layer of cobalt present between WC grains, its in situ deformation behavior during fracture is similar to the deformation of a thin ductile copper strip sandwiched between hard tool steel platens. In order to estimate the fracture toughness of cermets, this deformation analogy can be incorporated in Eq 13 for the constraint factor χ, through the relationship

$$\chi = \frac{\sigma_{eff}}{\sigma_0} = \left[1 + \frac{2k}{3}\left(\frac{d}{2h}\right)\right] \quad \text{(Eq 14)}$$

where σ_0 is the bulk flow stress of the binder in the absence of any constraint and σ_{eff} is the flow stress of the binder in situ in the microstructure. The constant k is defined as the maximum shear factor, which is taken as 0.577, and d and h are respectively the width of the rigid platen and the thickness of the ductile layer. In the case of cermets, as a first approximation, d and h can be considered to represent the mean WC particle diameter and the thickness of the cobalt binder, respectively. An increase in cobalt binder thickness and a decrease in WC particle size would therefore increase the constraint for deformation and hence the fracture toughness. Figure 25 compares experimental data with the theoretically calculated fracture toughness levels using Eq 13 and 14. The good correlation suggests that Eq 13 and 14 capture the effects of important microstructural parameters on the fracture toughness of cermets and can be used in the design of cermet composition and microstructure.

Metal-Matrix Composites. Light metals such as aluminum and magnesium are reinforced with particulates and whiskers based on SiC, Al_2O_3, TiC, and so on to increase the stiffness and high-temperature strength. These composites are made by dispersing reinforcements in liquid metal and casting or by mixing with metal powder and hot pressing. In general, the size and spacing of particles, the strength of the interface between the particles, and the aspect ratio of the whiskers influence the strength and fracture toughness of composites. Figure 26 illustrates the fracture toughness levels of aluminum alloys reinforced with second-phase particles, showing a decrease in fracture toughness at large particle volume fractions.

The fracture toughness of metal-matrix composites can be estimated approximately from:

$$K_{Ic} \propto \sqrt{E\,\sigma_y \varepsilon_f\, l^*} \quad \text{(Eq 15)}$$

where ε_f is the fracture strain of the ligament between the crack tip and the closest particle and l^* is the size of the process zone at the crack tip, usually taken as interparticle spacing. From this equation, it is clear that decreasing the interparticle spacing by increasing the volume fraction of dispersions reduces the fracture toughness of composites.

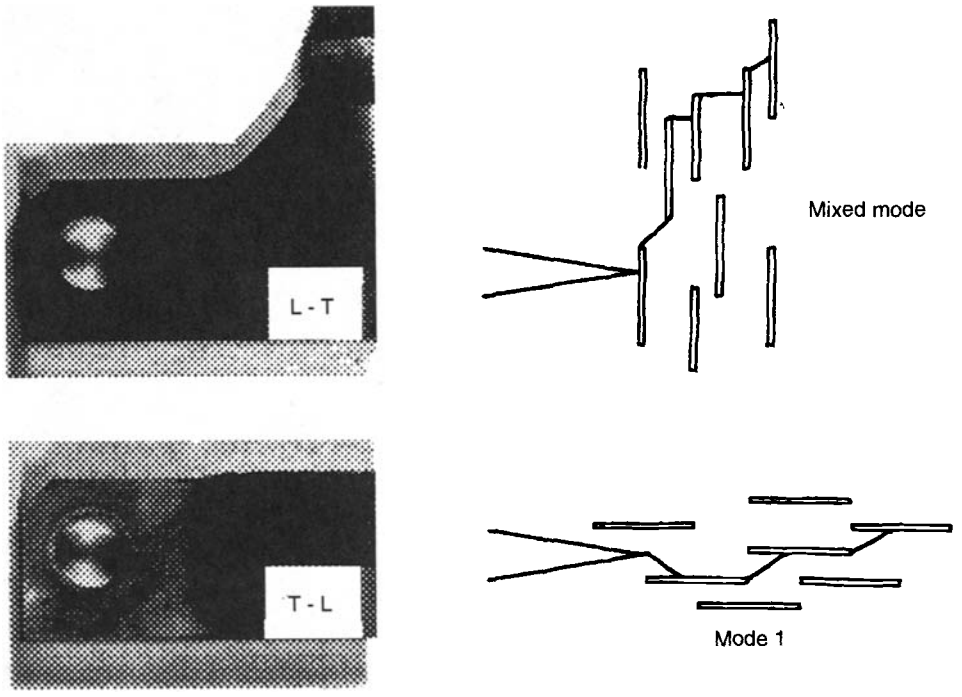

Fig. 28 Effect of whisker orientation on crack path and fracture in fracture toughness tests of 7075 + SiC-whisker composites

Figure 26 shows two composites, 6061 Al-Mg-Si alloy reinforced with various amounts of SiC particles and a rapidly solidified Al-Fe-V-Si alloy containing intermetallic particles. The trend is similar for both materials. There are two mechanisms by which reinforcements can affect fracture toughness. First, plastic flow localization at the interface and interface decohesion can significantly reduce the extent of void growth before ultimate failure, thus reducing fracture toughness. This is the case for the particulate composites. Alternatively, crack-tip blunting and crack path deviation around whiskers can increase fracture toughness by increasing the energy required for crack extension. However, for this to occur, the matrix-whisker interface must be strong. In reality, the interface is weaker due to reaction between the matrix and the whiskers during processing and the presence of oxides on the surfaces of whiskers. This effect is illustrated in Fig. 27, which shows that both orientations (whiskers oriented normal or parallel to crack plane) lead to a decrease in fracture toughness due to interface fracture. Figure 28 shows the crack path and whiskers are oriented differently with respect to the crack propagation direction in fracture toughness tests. The decrease in fracture toughness in the latter orientation is higher, due to increased weak interface area.

SELECTED REFERENCES

Basic Fracture Principles

- D. Broek, *Elementary Engineering Fracture Mechanics*, Kulewer Academic Publishers, 1986
- J.F. Knott, *Fundamentals of Fracture Mechanics*, Butterworths, London, 1973
- J.M. Kraft, Elastic-Plastic Fracture, *App. Mater. Res.*, Vol 3, 1964, p 88
- R.A. Wullaert, D.R. Ireland, and A.S. Telelman, Use of the Precracked Charpy Specimen in Fracture Toughness Testing, *Fracture Prevention and Control*, American Society for Metals, 1974, p 255

Steel

- A.J. Birkle, R.P. Wei, and G.E. Pellissier, *Trans. ASM*, Vol 59, 1966, p 981
- C.L.M. Cottrell, in *Fracture Toughness of High Strength Materials: Theory and Practice*, Publication 120, Iron and Steel Institute, London, 1970, p 112
- R.F. Decker, Alloy Design, Using Second Phases, *Metall. Trans.*, Vol 4, 1973, p 2495
- R.O. Ritchie and A.W. Thompson, On Macroscopic and Microscopic Analyses for Crack Initiation and Crack Growth Toughness in Ductile Alloys, *Metall. Trans.*, Vol 16A, 1985, p 233
- A.R. Rosenfield and A.J. McEvily, Some Recent Developments in Fatigue and Fracture, *Metallurgical Aspects of Fatigue and Fracture Toughness*, AGARD Report 610, NATO, 1973
- V.F. Zackay, Fundamental Considerations in the Design of Ferrous Alloys, *Alloy Design for Fatigue and Fracture Resistance*, AGARD Report 185, NATO, 1976, p 5.1
- V.F. Zackay and E.R. Parker, Fracture Toughness, *Alloy and Microstructure Design*, J.K. Tien and G.S. Ansell, Ed., Academic Press, 1976, p 213
- Z. Fan, The Grain Size Dependence of Ductile Fracture Toughness of Polycrystalline Metals and Alloys, *Mater. Sci. Eng.*, Vol A191, 1995, p 73
- S.D. Antolovich, A. Saxena, and G.R. Chanani, Increased Fracture Toughness in a 300 Grade Maraging Steel as a Result of Thermal Cycling, *Met. Trans.*, Vol 5, 1974, p 623

Aluminum Alloys

- J.D. Embury, Basic Microstructural Aspects of Aluminum Alloys and Their Influence on Fracture Behavior, *Alloy Design for Fatigue and Fracture Resistance*, AGARD Report 185, NATO, 1976, p 1.1
- G.C. Garrett and J.F. Knott, The Influence of Compositional and Microstructural Variations on the Mechanism of Static Fracture in Aluminum Alloys, *Metall. Trans.*, Vol 4A, 1978, p 1187
- G.T. Hahn and A.R. Rosenfield, Metallurgical Factors Affecting Fracture Toughness of Aluminum Alloys, *Metall. Trans.*, Vol 6A, 1975, p 653
- J.G. Kaufman, Design of Aluminum Alloys for High Toughness and High Fatigue Strength, *Alloy Design for Fatigue and Fracture Resistance*, AGARD Report 185, NATO, 1976, p 2.1
- A.K. Vasudevan, R.D. Doherty, and S. Suresh, Fracture and Fatigue Characteristics in Aluminum Alloys, *Aluminum Alloys-Contemporary Research and Applications*, A.K. Vasudevan and R.D. Doherty, Ed., Vol 31, *Treatise in Materials Science and Technology*, 1989, p 446

Titanium Alloys

- B.L. Averback, Microstructure and Fracture Toughness, *Fracture Prevention and Control*, American Society for Metals, 1974, p 97
- J.P. Hirth and F.H. Froes, Interrelations between Fracture Toughness and Other Mechanical Properties in Titanium Alloys, *Metall. Trans.*, Vol 8A, 1977, p 1165
- N.E. Paton, J.C. Williams, J.C. Chesnutt, and A.W. Thompson, The Effects of Microstructure on the Fatigue and Fracture of Commercial Titanium Alloys, *Alloy Design for Fatigue and Fracture Resistance*, AGARD Report 185, NATO, 1976, p 4.1
- K.H. Schwalbe, On the Influence of Microstructure on Crack Propagation Mechanisms and Fracture Toughness of Metallic Materials, *Eng. Fract. Mech.*, Vol 9, 1977, p 795
- C.A. Stubbington, Metallurgical Aspects of Fatigue and Fracture in Titanium Alloys, *Alloy Design for Fatigue and Fracture Resistance*, AGARD Report 185, NATO, 1976, p 3.1
- J.C. Williams, J.C. Chesnutt, and A.W. Thompson, The Effects of Microstructure on Ductility and Fracture Toughness of $\alpha+\beta$ Titanium Alloys, *Microstructure, Fracture Toughness and Fatigue Crack Growth Rate in Tita-*

nium Alloys, A.K. Chakrabarti and J.C. Chesnutt, Ed., TMS-AIME Publications, 1987, p 255

Composites and Cermets

- M.F. Ashby, F.J. Blunt, and M. Bannister, Flow Characteristics of Highly Constrained Metal Wires, *Acta Metall.*, Vol 37, 1989, p 1847
- A.G. Evans and R.M. McMeeking, *Acta Metall.*, Vol 34, 1988, p 2435
- K. Hirano, R & D Trends on Advanced Metal Matrix Composites and Fracture Mechanics Characterization, *ISIJ International*, Vol 32, 1992, p 1357
- F. Osterstock and J.L. Chermant, Some Aspects of the Fracture of WC-Co Composites, *Science of Hard Materials*, R.K. Viswanatham, D.J. Rowcliffe, and J. Gurland, Ed., Plenum Press, 1981, p 615
- K.S. Ravichandran, Fracture Toughness of Two Phase Composites based on WC-Co Cermets, *Acta Metall. Mater.*, Vol 42, 1994, p 143
- K.S. Ravichandran, A Survey of Toughness in Ductile Phase Composites, *Scripta Metall. Mater.*, Vol 26, 1992, p 1389
- K.S. Ravichandran and E.S. Dwarakadasa, An Overview of Structure Property Relationships in Advanced Aerospace Al Alloys, *J. Metals*, Vol 39, 1987, p 28
- V.V. Kristic, P.S. Nicholson, and R.G. Hoagland, Toughening of Glasses by Metallic Particles, *J. Am. Ceram. Soc.*, Vol 64, 1981, p 499